

# A numerical investigation on double-front detonation in solid explosive mixture with varying aluminum concentration

Wuhyun Kim, Min-cheol Gwak, and Jack J. Yoh\*

Department of Mechanical & Aerospace Engineering, Seoul National University  
Seoul, Korea 151-742

## 1 Introduction

The performance characteristics of the aluminized high explosive is considered using the various aluminum (Al) concentration in the hybrid non-ideal detonation model. Since there exist differences in the time scales of the characteristic induction and combustion of high explosives and Al particles, the process of energy release behind the leading detonation wave front occurs over an extended period of time. Subsequently, the decrease in detonation velocity with increasing Al concentration and the double-front detonation (DFD) feature when anaerobic Al reaction occurs behind the front are the two cardinal observations reported. In order to simulate the performance characteristics associated with varying Al concentration within HMX base charge, the multiphase conservation laws are formulated for mass, momentum, and energy exchange between Al particles and HMX product gases. Here, two-phase model (KV model) [1] is implemented into a hydrocode that simulates a series of unconfined and confined rate stick tests. The simulated results are compared with the experimental data for 5-25% concentrations [2], and the formation of DFD structure under varying Al concentration (0-50%) in HMX is investigated.

## 2 Numerical formulation

To solve the aluminized HMX reaction problem using in-house hydrocode with mesh resolution of 1/10 mm, we use the third-order Convex ENO method and the third-order Runge-Kutta (RK) method for spatial integration and time integration, respectively. Based on the multiphase conservation laws with the interaction effects considered, the governing equations in an axisymmetric cylindrical ( $\varphi=1$ ) and rectangular ( $\varphi=0$ ) coordinates are constructed as Eqs. (1)-(6).

$$\frac{\partial S}{\partial t} + \frac{\partial F}{\partial x} + \frac{\partial G}{\partial y} = RHS \quad (1)$$

$$S = [\rho, \rho v_1, \rho v_2, \rho E_{HMX}, \rho \lambda, \sigma, \sigma u_1, \sigma u_2, \sigma E_{Al}]^T \quad (2)$$

$$F = [\rho v_1, \rho v_1^2 + P, \rho v_1 v_2, v_1 (\rho E_{HMX} + P), \rho \lambda v_1, \sigma u_1, \sigma u_1^2, \sigma u_1 u_2, u_1 \sigma E_{Al}]^T \quad (3)$$

$$G = [\rho v_2, \rho v_1 v_2, \rho v_2^2 + P, v_2 (\rho E_{HMX} + P), \rho \lambda v_2, \sigma u_2, \sigma u_1 u_2, \sigma u_2^2, u_2 \sigma E_{Al}]^T \quad (4)$$

$$RHS = \begin{bmatrix} \dot{\sigma}, \dot{\sigma} u_1 - \dot{f}_1, \dot{\sigma} u_2 - \dot{f}_2, -\dot{Q}_H + \dot{\sigma} E_{Al} + \dot{\sigma} \Delta H - \dot{f} \cdot \bar{u}, \rho \dot{w}_{HMX}, \\ -\dot{\sigma}, -\dot{\sigma} u_1 + \dot{f}_1, -\dot{\sigma} u_2 + \dot{f}_2, \dot{Q}_H - \dot{\sigma} E_{Al} + \dot{f} \cdot \bar{u} \end{bmatrix} + R \quad (5)$$

$$R = -\frac{\phi}{x} [\rho v_1, \rho v_1^2, \rho v_1 v_2, v_1 (\rho E_{HMX} + P), v_1 \lambda, \sigma u_1, \sigma u_1^2, \sigma u_1 u_2, u_1 \sigma E_{Al}]^T \quad (6)$$

where  $\lambda$ ,  $\rho$ ,  $\sigma$ ,  $v$ ,  $u$ ,  $\psi$ ,  $\rho_{Al}$ ,  $\dot{w}_{HMX}$ ,  $P$ ,  $E$ ,  $Re$ ,  $C_D$ ,  $Nu$ , and  $d_p$  are production mass fraction, diluted HMX density, diluted Al particle density, HMX product gas velocity, Al particle velocity, volume fraction of gaseous components able to oxidize Al, aluminum density, reaction rate of HMX, pressure, specific total energy, Reynolds number, drag coefficient, Nusselt number, and diameter of initial Al particle, respectively.

The exchanges of physical quantities are determined as Eqs. (7)-(13) [1]. Then, the burning time of an individual particle follows the empirical law [3] which considers the amount of oxidizing species for Al particle, and the heat of reaction of Al ( $\Delta H = 13410$  kJ/kg) is referred from the experiment [4].

$$\dot{\sigma} = \frac{3\sigma}{t_b} (1.0 + 0.276\sqrt{Re}) ; T_p \geq T_{ign}, \quad else \quad \dot{\sigma} = 0 \quad (7)$$

$$t_b = K d_p^2 / \psi^{0.9} \quad (8)$$

$$\dot{f} = \frac{3}{4} \frac{\rho}{\rho_{Al}} \frac{\sigma}{d_p} C_D (v-u) \|v-u\| \quad (9)$$

$$C_D = \frac{24}{Re} + \frac{4.4}{\sqrt{Re}} + 0.42 \quad (10)$$

$$Re = \frac{\rho d_p \|v-u\|}{\mu} \quad (11)$$

$$\dot{Q}_H = \frac{6\sigma Nu k_g (T_{HMX} - T_{Al})}{\rho_{Al} d_p^2} \quad (12)$$

$$Nu = 2.0 + 0.459 Re^{0.55} Pr^{0.33} \quad (13)$$

The Al temperature is calculated from the thermodynamic identity of bulk scale Al, and conductivity ( $k_g$ ), Prandtl number ( $Pr$ ), viscosity ( $\mu$ ) of burned explosive properties are calculated from curve fitting by the NASA CEA (Chemical Equilibrium with Applications) code [5]. Also  $K = 1.894 \times 10^6$  s/m<sup>2</sup> is considered in the burning time,  $t_b$ .

For numerical simulation of detonation, the reaction model and equation of state (EOS) are adapted from ignition and growth (I&G) model and JWL EOS for PBX 9501 (95% HMX/5% -Estane, BDNPA/F) [6].

### 3 Results and Discussion

The simulation objective is the performance assessment of varying Al concentration in an aluminized HMX with fixed particle size 7  $\mu$ m. Two main features of interest in the analysis include i) the DFD structure which is resulted from burning of Al particles behind the leading detonation front, and ii) the decrease in detonation velocity with increasing Al concentration. To reproduce DFD structure, unconfined rate stick of 40 mm diameter and 45 mm length are considered as shown in Fig. 1(a), which is the same condition from the experiment [2]. As for confined rate stick test, diameter of 20 mm and length of 100 mm is considered as in Fig. 1(b). This test is meant to observe the decrease in detonation velocity as reported from the experiment [2]. The confiner thickness is 2 mm using copper. The simulation using in-house hydrocode The

boundary between the two materials is partitioned using a level-set method, and the interface is represented by a solid line as a zero level-set. A full description of the interface handling technique is referenced in [7].

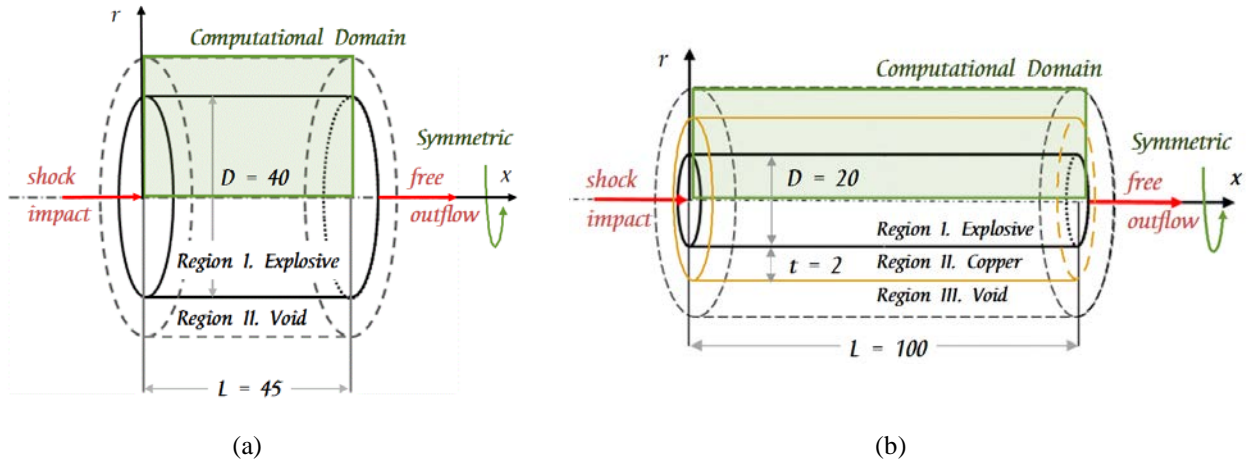


Fig. 1 Computational domains of two dimensional cylindrical rate stick tests: (a) unconfined rate stick and (b) 2 mm-copper confined rate stick

**Unconfined rate stick test - Double-front detonation of aluminized HMX**

The unconfined rate stick test of [2] is simulated. Figure 2 shows pressure history of non-aluminized HMX and 15% aluminized HMX at the end of the rate stick, in comparison to experimental measurement. The double front structure also appears when aluminum is present that results in the secondary peak pressure delay behind the leading detonation front.

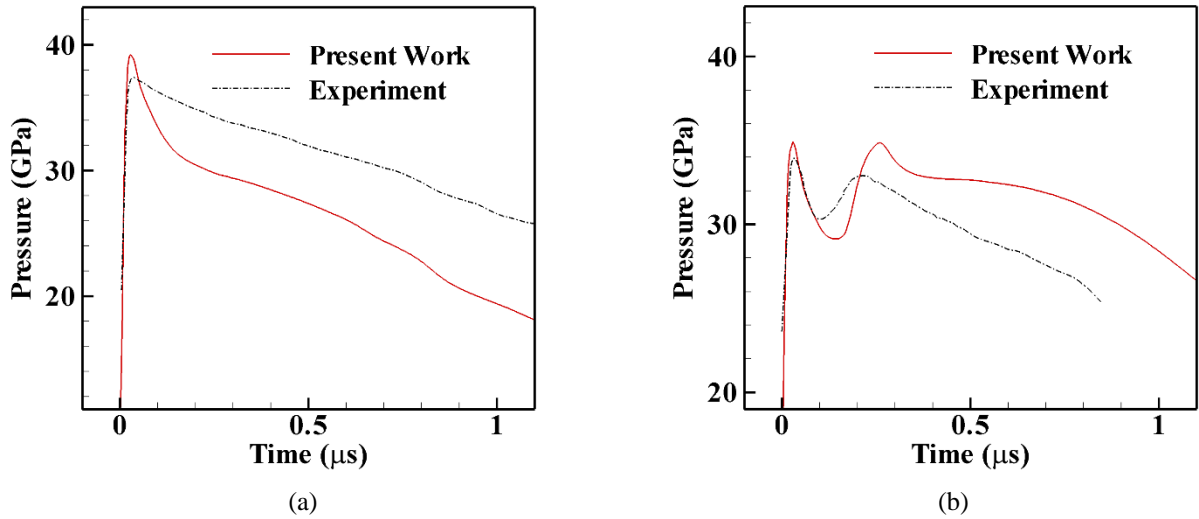


Fig. 2 Comparison between experiment data and simulation for pressure in (a) non-aluminized 95% HMX and (b) 15% aluminized HMX

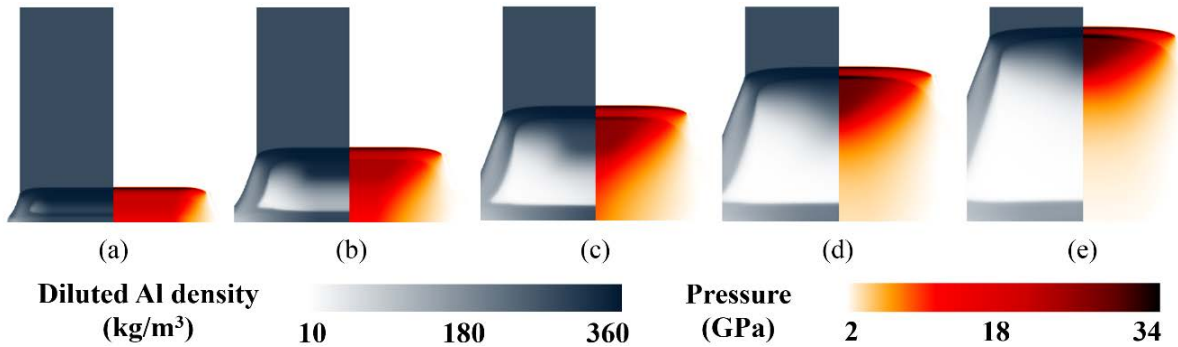


Fig. 3 Density of diluted Al particles and pressure contours of 15 % aluminized HMX unconfined rate stick simulation at (a) 1  $\mu$ s, (b) 2  $\mu$ s, (c) 3  $\mu$ s, (d) 4  $\mu$ s and (e) 5  $\mu$ s after shock impact

In Fig.3, the detonation propagation in aluminized HMX (15% Al concentration) is shown using the density of diluted Al particles and the pressure field. Since high explosives and Al particles have different ignition delay time, the burning process of Al particles takes place behind the leading detonation front over a relatively long time period. Consequently, DFD is generated and becomes distinct over time.

#### Confined rate stick test - Detonation velocity of aluminized HMX

The detonation velocity of aluminized HMX is studied using the confined rate stick test of Fig. 1(b). In Figure 4(a) representing steady propagation pressure profiles, one confirms that the detonation velocity decreases with the increase in the concentration of Al particles. This is shown by varying the Al concentration from 0 to 25% and taken at 6  $\mu$ s. The steady propagation detonation velocity is decreased from 8823 m/s at zero Al concentration to 8533 m/s at 25% concentration. In addition, the double front structure starts to appear when the concentration is higher than 5%. At 25%, DFD is formed quite clearly as the second peak pressure increases.

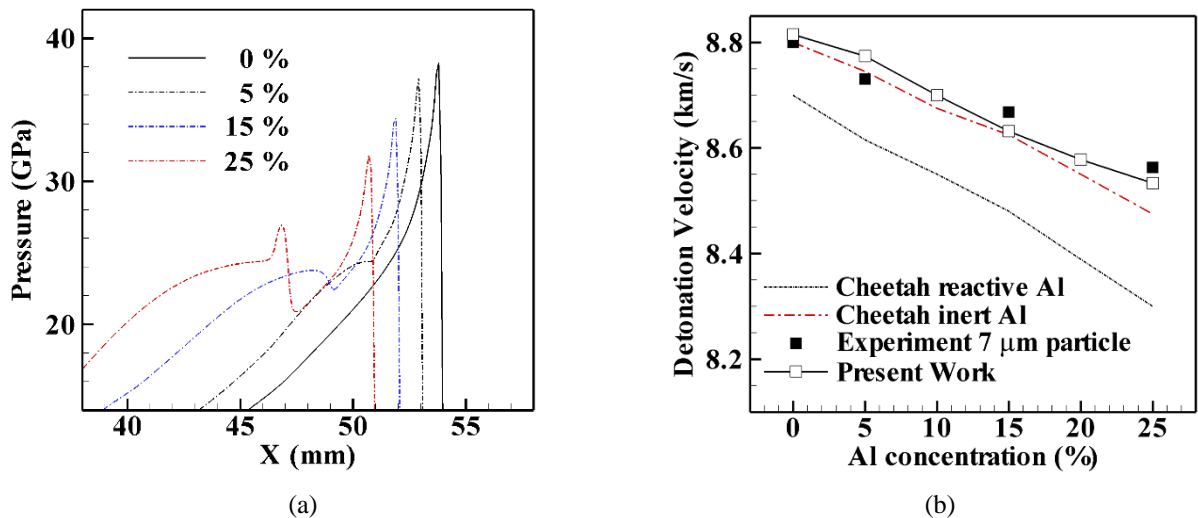


Fig. 4 (a) Comparison of detonation profiles of aluminized HMX with different Al concentration (0, 5, 15, and 25%) and constant particle size 7  $\mu$ m taken at 6.0  $\mu$ s after shock impact. (b) Detonation velocity versus Al concentration from Cheetah calculation, experiment [2], and present simulation

In Fig. 4(b), Cheetah calculation [8], experiment [2], and simulation results are compared using detonation velocity with Al concentration. The experiment covered three specific concentrations of 5, 15,

and 25%, while Cheetah and present simulation considered five concentrations (5, 10, 15, 20, 25%). As seen in the experimental data in figure 4(b), the detonation velocity decreases with Al concentration increase. There are two important factors responsible for the decrease of detonation velocity. First is the lowered mass of the HMX in the mixture when Al is increased. Subsequently the detonation energy of the mixture is lowered. Second is the loss of momentum and energy starting from the leading shock front due to interaction of Al particles with detonation products. The calculated detonation velocity follows precisely the experimental data. Two Cheetah calculations are also shown. The reactive Al case uses Wood-Kirkwood reaction model while the inert Al case is the standard Cheetah run with Al concentration variation. Although ignition delay and energy dissipation can be estimated, Cheetah cannot simulate the DFD structure based on the momentum and energy exchange between Al particles and explosive products. For this reason, the present model is used to quantify the experimental data with varying Al concentration in Fig. 4(b).

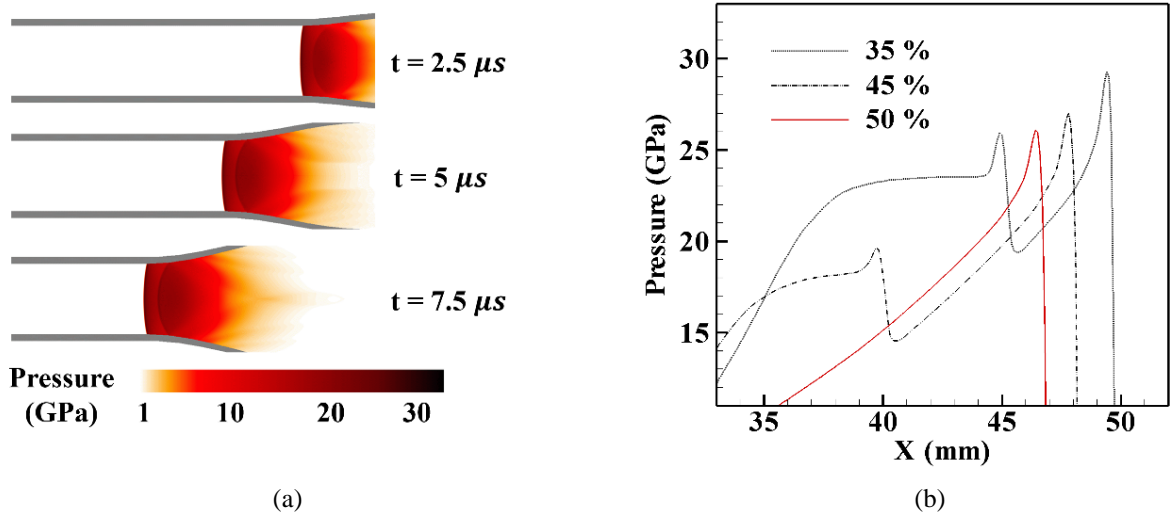


Fig. 5 (a) Pressure contours of 25% aluminized HMX in confined rate stick simulation, and (b) comparison of detonation profiles of aluminized HMX with 35, 45, and 50% Al concentration, taken at  $6 \mu s$  after shock impact

Figure 5(a) depicts pressure contours in a confined rate stick that account for the detonation of 25% aluminized HMX with constant particle size,  $7 \mu m$ . Here, the calculated detonation propagation velocity is  $8533 \text{ m/s}$ , which is close to the experimental value of  $8563 \text{ m/s}$ . Also the second peak is shown due to a burning of Al particles behind the detonation spike of the explosive.

#### Confined rate stick test – “Heavily” aluminized HMX (35~50% Al concentration)

From Fig. 4(a), it was shown that the formation of DFD becomes evident as Al concentration is raised from 0 to 25%. The presence or disappearance of the DFD structure has not been addressed from the previous experiments reported in the literature. For this reason, we consider higher Al concentration beyond the experimentally tested limit under the same test geometry (confined rate stick test). Figure 5(b) depicts the detonation structure when Al concentration is raised from 35% to 50%. Unlike the results in Fig. 4(a), pressure histories of heavily aluminized HMX show that the second peak pressure decreases for Al concentration increase from 35% to 45%. When the Al concentration reaches 50%, the DFD structure disappeared and attenuated normal detonation wave is obtained. Accordingly, as the total energy of the reacted HMX decreases with more Al concentration, there exists insufficient energy necessary to ignite the Al particles in the reaction plume. As shown in Eq. 12, the insufficient energy of HMX product gases invites the incompetent energy exchange rate for heating up Al particles. From that reason, in case of the excessively aluminized explosive shown at the result of 50% Al, the relevant ignition temperature is never reached and

the burning of Al particles is no longer possible. To avoid such inefficiency, the aluminum concentration in aluminized HMX is commonly not to exceed 35%.

## 4 Conclusion

A hydrodynamic simulation using KV model is utilized to understand the effect of aluminum concentration in the aluminized HMX. The double front structure of the steady state detonation is observed while the decrease in the detonation velocity is observed with increasing aluminum concentration. The results are quantified via the available experimental data. The presented method is suitable for predicting the non-ideal high explosive characteristics such as detonation velocity, pressure, and temperature in accordance with the aluminum concentration variation.

## Acknowledgment

This work was financially supported by Agency for Defense Development (ADD) contracted through IAAT and Basic Science Research Program (2016R1A6A3A11932827) funded by the Ministry of Education. Additional support from the Next Generation Space Propulsion Research Center at Seoul National University is warmly acknowledged.

## References

- [1] Veyssiere B., Khasainov BA. (1991). A model for steady, plane, double-front detonations (DFD) in gaseous explosive mixtures with aluminum particles in suspension, *Combust. Flame.* 85: 241
- [2] Zhang F. (2009). *Shock Wave Science and Technology Reference Library*. Springer. 4: 217
- [3] Price EW. (1984). Combustion of metalized propellants. *Prog. Astronaut. Aeronaut.* 90:479
- [4] Makhov M., Gogulya M., Dolgoborodov A., Brazhnikov M., Arkhipov V., Pepekin V. (2004). Acceleration Ability and Heat of Explosive Decomposition of Aluminized Explosives. *Combust. Explos. Shock Waves.* 40: 458
- [5] McBride BJ., Gordon S. (1992). Computer Program for Calculating and Fitting Thermodynamic Functions. NASA Rept. RP-1271.
- [6] Tarver C. M. (2015). Ignition and Growth Reactive Flow Modeling of Recent HMX/TATB Detonation Experiments. 19th Biennial APS-SCCM.
- [7] Kim K., Yoh J. J. (2012). A particle level-set based Eulerian method for multi-material detonation simulation of high explosive and metal confinements. *Proc. Combust. Inst.* 34: 2025
- [8] Fried L. E., Glaesemann K. R., Howard W. M., Souers P. C., Vitello P. A. (2004), CHEETAH 4.0 User's Manual, UCRL-CODE-155944, Lawrence Livermore National Laboratory.